EASR

Engineering and Applied Science Research

https://www.tci-thaijo.org/index.php/easr/index

Published by the Faculty of Engineering, Khon Kaen University, Thailand

Design and fabrication of a low-cost research facility for the study of combustion characteristics of a dual producer gas-diesel engine

Monorom Rith*[1, 2)], Bernard Buenconsejo[3)], H.W. Gitano-Briggs[4)] and Jose Bienvenido Manuel M. Biona[1,5)]

[1)]Mechanical Engineering Department, De La Salle University, 1004 Metro Manila, Philippines
[2)]Research and Innovation Center, Institute of Technology of Cambodia, Russian Conf. Blvd, Phnom Penh, Cambodia
[3)]Department of Total Sensing Solutions, Keyence Philippines Inc., 1004 Metro Manila, Philippines
[4)]Mechanical Engineering Department, Universiti Kuala Lumpur Malaysian Spanish Institute, Kedah, Malaysia
[5)]Enrique K. Razon Jr. Logistics Institute, De La Salle University, LTI Spine Road, Laguna Blvd, Biñan, Laguna 4024, Philippines

Received 8 March 2020
Revised 14 May 2020
Accepted 15 May 2020

Abstract

A combustion pressure measurement system is a major unit used to study combustion characteristics of an alternative fuel compared to a baseline fossil fuel. Many previous studies have used a Kistler make transducer connected to a Kistler charge amplifier to detect the combustion pressure inside the cylinder, but the prices are very high, more than 5,000 US$. Consequently, this technical paper provides some tips to properly assemble a combustion pressure measurement system with a much lower price and apply theoretical functions to convert raw data into combustion output variables. An AutoPSI pressure sensor connected with a charge amplifier and a PicoLog 1012 data logger was chosen, and the total cost was 2,250 US$. The pressure measurement unit was used to detect the combustion pressure of producer gas in a diesel engine operated in dual fuel mode. A venturi and a U-tube manometer were designed and fabricated to read producer gas flow rates based on the Bernoulli principle. Three different engine loads (i.e., 35%, 53%, and 70%) with gas flow rates (i.e., no gas, 10 kg/h, and 20 kg/h) were controlled to test the combustion pressure measurement system and the gas flow reader. The results highlighted that the combustion characteristics of the present study are in the same trends as those of existing studies. The combustion peak occurs lower and later with a higher gas flow rate, but an increase in engine load raises the peak pressure. This study contributes to offering technical tips to design a low-cost research facility.

Keywords: Pressure sensor, Gas flow reader, Syngas, Fuel combustion, Compression ignition engine, Dual fuel

1. Introduction

An increase in fossil fuel price, petroleum reservoir depletion, and air pollution have caused a growing interest in research of alternative fuel exploitation for internal combustion (IC) engine to diminish diesel and gasoline dependency and reduce atmospheric pollutant emissions. Compressed natural gas (CNG), liquefied petroleum gas (LPG), Hydrogen (H_2), and liquefied or gaseous biofuels have been extensively utilized to study the engine performances and emissions and then compared with the gasoline or the diesel as the baseline [1-8], and other some literature studied the reduction in fuel gas emissions [9-10]. Investigation of engine performance and emission characteristics does not require any internal modification of an engine [11-12]. However, the study of engine combustion characteristics needs a pressure sensor or pressure transducer installed on the cylinder head to firstly detect combustion pressure that is recorded by a data acquisition system. Then, the raw combustion pressure data are converted into the profiles of combustion pressure, net heat release rate (NHRR), cumulative heat release (CHR), ignition delay, and combustion duration [6, 13]. Correspondingly, the combustion characteristics of alternative fuels can be investigated and compared with fossil fuels considered as the baselines. Many previous studies have used a Kistler make transducer connected to a Kistler charge amplifier to study the combustion characteristics. However, the prices of this toolkit are very high, more than 5,000 US$. Many academics and graduate students in developing countries are unable to purchase these tools for research and experiment. Therefore, this study introduces another pressure sensor connected with a charger amplifier and a medium speed data acquisition system at a much lower price. The authors also show how to assemble the combustion pressure measurement system and visualize the combustion output variables.

*Corresponding author. Tel.: +63 966 480 9818
Email address: rith_monorom@dlsu.edu.ph
doi: 10.14456/easr.2020.48

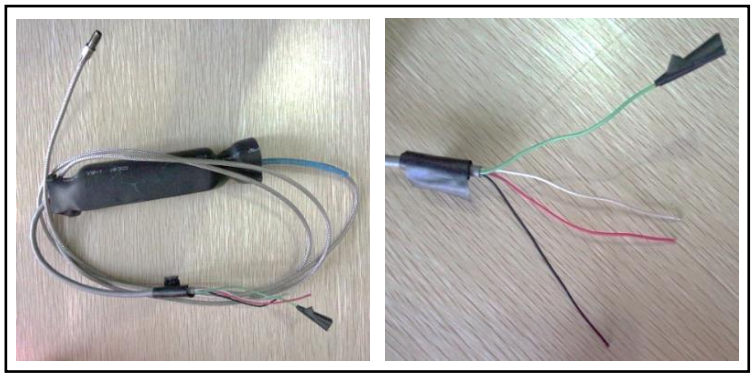

Figure 1 AutoPSI pressure sensor (left) and its different color-coded leads (right)

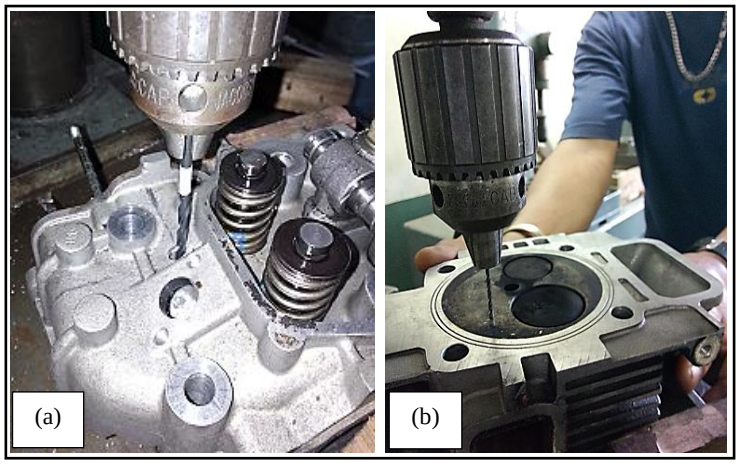

Figure 2 Drilling a hole: a) on the top of the cylinder head, and b) on the bottom of the cylinder head

Producer gas or syngas is a gaseous fuel converted from biomass through a thermochemical process. This gas is considered a renewable technology for the exploitation of agricultural residues. In our study, producer gas was used to partially replace diesel fuel to study the combustion characteristics of a dual fuel mode and compared with the neat diesel mode. Gas flow rates have a significant impact on combustion characteristics [11, 13-15]. However, the gas flow rate reader is not commercially available. Many previous studies have investigated the combustion characteristics at the maximum diesel replacement rate [7, 15-16]. Therefore, this technical report provides some technical tips to design a gas flow rate reader based on the Bernoulli principle. Based on the existing literature, there is no study of designing a reader for producer gas flow rates. The contribution of this study is twofold: 1) an assembly of a combustion pressure measurement system with a much lower price and 2) the design of a gas flow rate reader. This article is highly expected to be informative for graduate students in developing countries having research budget constraints for the study of alternative fuels and internal combustion engines. Furthermore, the concept of designing a gas flow rate reader can also be applied for a reader for other gaseous fuels such as biogas, natural gas, and LPG. The novelty of this study is the provision of technical tips to design a low-cost research facility for the study of the combustion characteristics of alternative gaseous fuel.

2. Installing a pressure sensor on a cylinder head

2.1 Specifications of the pressure sensor

An AutoPSI pressure sensor connected to a charge amplifier was taken to design a low-cost research facility to study engine combustion characteristics because the price is only 2,000 US$. The pressure sensor is presented in Figure 1. The sensor element was coupled to an enclosure through an optical fiber. The enclosure houses all the electronic circuitry and consists of leads coded in four colors to terminate a power source and a data acquisition system. The function of each wire is described as follows [17]:

- White: Sensor output signal;
- Green: Diagnostic, static calibration;
- Red: Power; and
- Black: Ground (power and signal).

Something surrounded by the biggest black hose is the charge amplifier of the sensor, as seen in Figure 1 (left). The specifications of the sensor are detailed in Appendix 1. The pressure sensor mounted on the engine cylinder head to measure the dynamic combustion pressure is described in the next subsection.

2.2 Mounting the pressure sensor on the engine cylinder head

The pressure sensor was mounted on the cylinder head of a KM 168 diesel engine. The technical specifications of the engine are detailed in Appendix 2. The thickness of the cylinder head casing is approximately 17 mm. The cylinder head, beforehand, was removed out of the engine. In the beginning, an 8-mm drilling bit was used to drill the casing of air cooling above the cylinder with a through-hole, as illustrated in Figure 2 (left). Then, the cylinder head was

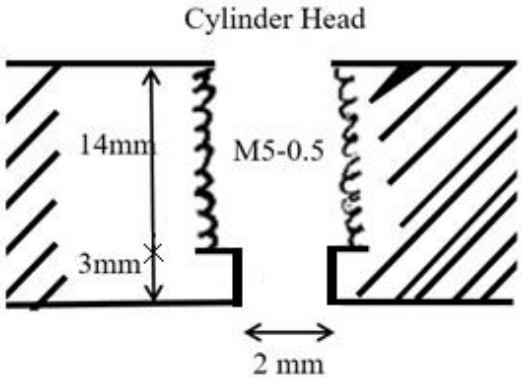

Figure 3 Mechanical drawing of the hole with thread for placing the pressure sensor

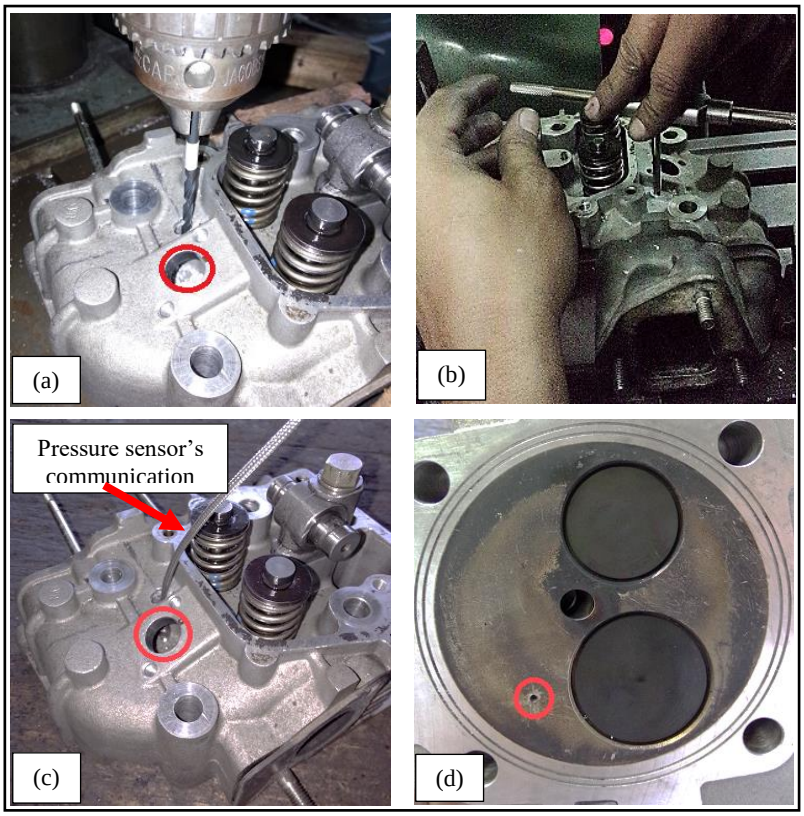

Figure 4 The photographic view of mounting the pressure sensor on the cylinder head: a) drilling a hole, b) making a thread, c) mounting a pressure sensor, and d) a hole for a pressure sensor tip

drilled through using a 2-mm drilling bit from the bottom surface. Subsequently, a 4.5-mm drilling bit was used to drill the same hole of the cylinder head from the air cooling casing. The depth of drilling the cylinder head is 14 mm for making the thread (as illustrated in Figure 3).

After that, an M5–0.5 hand tap was used to make the thread (see Figure 4, top right corner), and the pressure sensor was threaded in the hole (see Figure 4, bottom left corner). Look at the red oval circles highlighted on the figure (bottom right corner), the mounted pressure sensor is close to the intake valve, and the fuel combustion pressure is detected by the pressure sensor fixed to the 2-mm diameter drilled hole.

3. Connecting a pressure sensor and a crank angle sensor to a data acquisition system

Combustion pressure and crank angle must be recorded simultaneously. Therefore, the combustion pressure can be plotted in terms of the crank angle.

3.1 Pressure sensor

The pressure sensor was used to measure the dynamic pressure of fuel combustion. The green color wire was not used because it is designed for static pressure calibration. Figure 5 presents the connection of each wire to a data logger's terminal board and a power supply. The red color wire was connected to a 12V DC power supply, the black wire was fixed with the ground port of the terminal board and the ground wire of the power supply, and the white color-coded lead was screwed to channel 1 of the terminal board. The terminal board was directly interfaced with the data logger connected to a laptop using the communication cable.

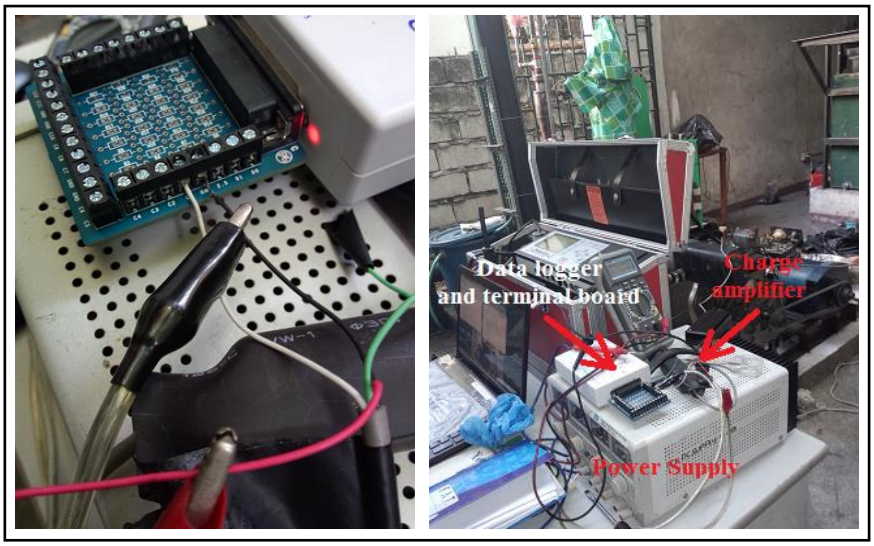

Figure 5 Wires of a charge amplifier connected to a data logger terminal board

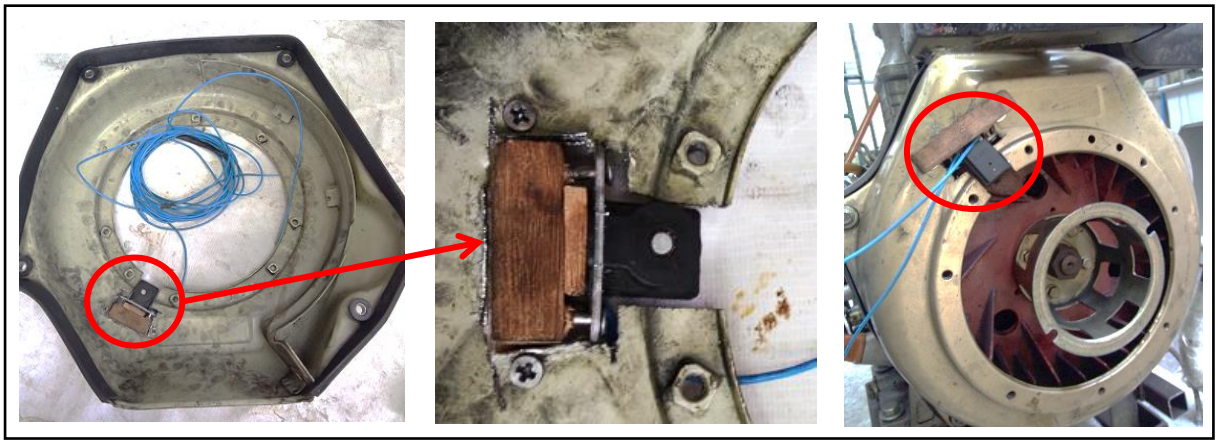

Figure 6 An inductive type sensor mounted on a fan casing to detect fan blades

3.2 Crank angle sensor

An inductive type speed sensor was mounted on the casing of the engine fan blades to detect the fan blades, as illustrated in Figure 6. The voltage source of the sensor is 12 V DC. The terminal board of the data logger is designed for a sensor with a power output of 0 through 2.5 V. A voltage divider was used (see Figure 7); otherwise, the sensor cannot be connected directly to the terminal board.

3.3 Data acquisition system

The data acquisition system is composed of a terminal board, a data logger, and a USB cable (as illustrated in Figure 8). The terminal board allows the sensor wires to attach the data logger without soldering. In this technical article, we used a PicoLog 1000 series, 1012 modal data logger to record data. The cost of the data logger was approximately 250 US$ (tax included). The PicoLog data logger is designed to record data at medium speed with multichannel voltage-input. The data logger is connected to a personal computer (PC) that can visualize the data in terms of time. This data logger can be used to record the dynamic combustion pressure and crank angle simultaneously. The specifications of the data logger are listed in Appendix 3.

4. Design and fabrication of a producer gas flow reader

A venturi and a U-tube manometer were designed to measure gas flow rates. The gas is compressible, but it was assumed to be a non-compressible fluid as its flow rate was low, roughly 12.14 m^3/h [18]. Additionally, the streamline is inviscid and steady. It is possible to apply the Bernoulli equation between any two points on the streamline:

$$\frac{P_1}{\gamma}+\frac{V_1^2}{2g}+h_1=\frac{P_2}{\gamma}+\frac{V_2^2}{2g}+h_2 \quad (1)$$

where P_1: Static pressure at position (1) (N/m^2)
P_2: Static pressure at position (2) (N/m^2)
γ: Specific weight (N/m^3)
g: Gravity acceleration $(9.81\ m/s^2)$
h_1: Height at position (1) (m)
h_2: Height at position (2) (m)
V_1: Fluid velocity at position (1) (m/s)
V_2: Fluid velocity at position (2) (m/s)

$$\Leftrightarrow \quad V_1^2-V_2^2=\frac{2g(P_2-P_1)}{\gamma}=\frac{2(P_2-P_1)}{\rho}$$

but $$P_2-P_1=\rho_{H_2O}gh \quad (2)$$

$$V_2=\frac{D_1^2}{D_2^2}V_1 \quad (3)$$

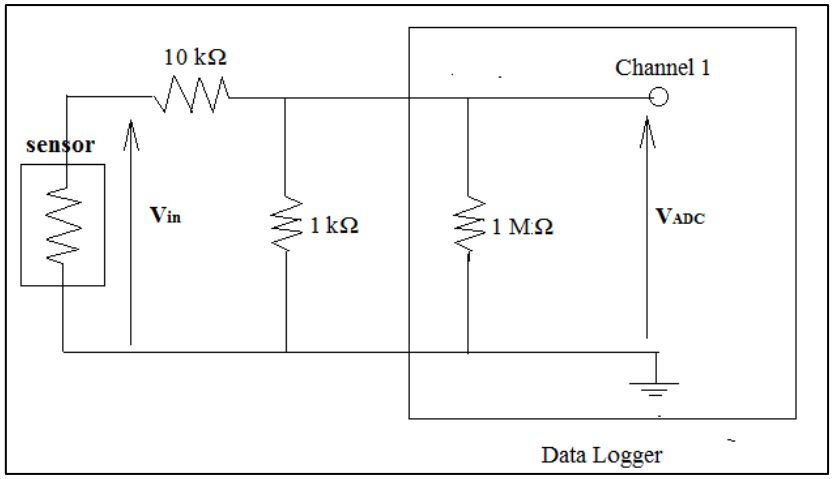

Figure 7 Schematic diagram of a voltage divider for the speed sensor

Figure 8 PicoLog 1000 series, 1012 modal, data logger

where ρ: Producer gas density (kg/m^3)
h: a different height of manometric fluid (m)

$$\Leftrightarrow \quad V_1^2 - \left(\frac{D_1^2}{D_2^2}V_1\right)^2 = \frac{2(\rho_{H_2O}gh)}{\rho}$$

$$\Rightarrow \quad V_1 = \sqrt{\left(\frac{D_2^4}{D_2^4 - D_1^4}\right)\left[\frac{2(\rho_{H_2O}gh)}{\rho}\right]} \qquad (4)$$

$$\Rightarrow \quad \dot{V} = \frac{\pi D_1^2}{4}\sqrt{\left(\frac{D_2^4}{D_2^4 - D_1^4}\right)\left[\frac{2(\rho_{H_2O}gh)}{\rho}\right]} \qquad (5)$$

$$\Rightarrow \quad \dot{m} = \rho\dot{V} \qquad (6)$$

where $\dot{V}$: Volumetric flow rate (L/min)
$\dot{m}$: Mass flow rate (kg/h)

The water at a temperature of 20℃ was used as the manometric fluid in our study, and its density is $\rho =$ 998.2 kg/m^3 [19]. The density of the gas was assumed to be constant because its relative pressure was low, based on the pre-test of our study. Furthermore, the varied percentage of the gas density at the atmospheric pressure compared to that of the actual pressure was less than 1.5% only when the gas flow rate was maximum. The presentation of the producer gas as an example based on the ideal gas law is shown below:

$$P_{absolute}V = mR_{specific}T \Rightarrow \rho_{specific} = \frac{m}{V} = \frac{P_{absolute}}{R_{specific}T} \quad (7)$$

$$R_{specific} = \frac{R}{M} \qquad (8)$$

where $R = 8.314$ Nm/K mol is the ideal gas constant. For the producer gas, $M_{producer\ gas}$ is the molar mass of the producer gas. The gas was assumed to be composed of 17.50% CO, 12.5% H_2, 15% CO_2, 3% CH_4, and 52% N_2 [18].

$$M_{producer\ gas} = \frac{(17.50\times CO)+(12.5\times H_2)+(15\times CO_2)+(3\times CH_4)+(52\times N_2)}{100} \qquad (9)$$

$$M_{producer\ gas} = \frac{(17.50\times 28)+(12.5\times 2)+(15\times 44)+(3\times 16)+(52\times 28)}{100} = 26.79 \text{ g/mol}$$

$$\Rightarrow R_{specific} = \frac{8.314 \text{ Nm/K mol}}{26.79 \text{g/mol}} = 0.310 \text{ Nm/g k} = 310 \text{ Nm/kg K}$$

According to the pre-test, the different height of the manometric water in the U-tube manometer at the maximum engine load is 40 mm, and the corresponding gas temperature was 30℃. Thus, the absolute pressure is 100,933 N/m^2, according to equation (10) below.

$$P_{absolute} = \rho_{H_2O}gh \qquad (10)$$

$$\Rightarrow \rho_{specific}\ (producer\ gas) = \frac{100{,}933 \text{ N/m}^2}{310 \text{ Nm/kgk} \times 303\text{K}} = 1.075\text{kg/m}^3$$

but $\rho_{atm}\ (producer\ gas) = 1.09\text{kg/m}^3$

$$\Rightarrow \frac{\rho_{\text{atm}}\ (\text{producer gas}) - \rho_{\text{specific}}\ (\text{producer gas})}{\rho_{\text{atm}}\ (\text{producer gas})} = \frac{1.09 - 1.075}{1.09} = 1.37\%$$

The venturi and the U-tube manometer were designed to read the producer gas flow rate, and the water was used as the manometric fluid, as mentioned earlier. The density of the gas at 27℃ was assumed to be 1.09 kg/m^3 [18]. This

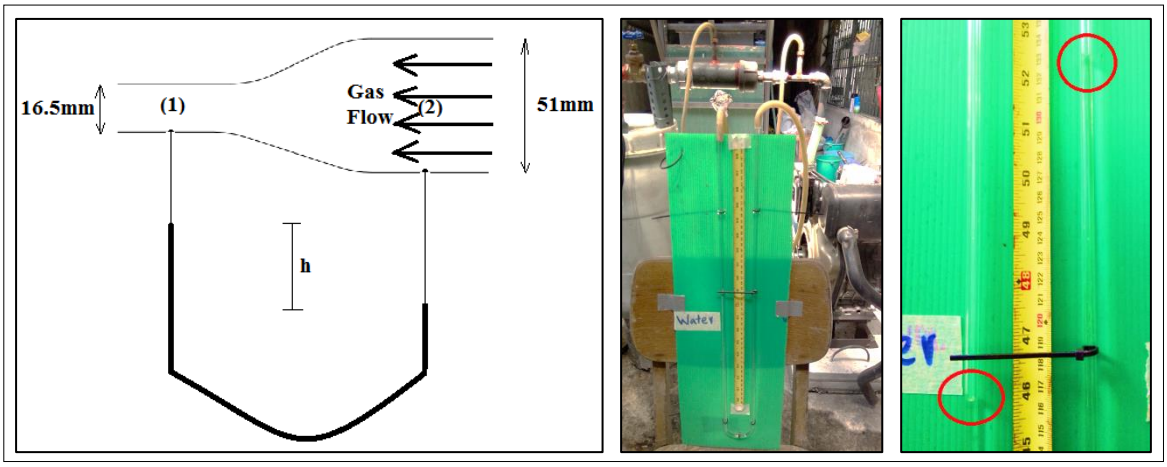

Figure 9 A venturi and U-tube manometer

Table 1 Volumetric and mass flow rates of producer gas

h(mm)	V̇(L/min)	ṁ(kg/h)
0	0.00	0.00
0.5	38.64	2.53
1	54.64	3.57
1.5	66.93	4.38
2	77.28	5.05
3	94.65	6.19
4	109.29	7.15
6	133.85	8.75
8	154.56	10.11
10	172.80	11.30
12	189.29	12.38
14	204.46	13.37
16	218.58	14.29
18	231.84	15.16
20	244.38	15.98
22	256.30	16.76
24	267.70	17.51
26	278.63	18.22
28	289.15	18.91
30	299.30	19.57
32	309.11	20.21
34	318.63	20.84
36	327.86	21.44
38	336.85	22.03
40	345.60	22.60
42	354.13	23.16
44	362.47	23.70
46	370.61	24.24
48	378.59	24.76
50	386.39	25.27
52	394.04	25.77
54	401.55	26.26
56	408.92	26.74
58	416.16	27.21
60	423.27	27.68
62	430.27	28.14
64	437.15	28.59
66	443.93	29.03
68	450.61	29.47
70	457.19	29.90
72	463.67	30.32

assumption was informative to calculate gas flow rates because the gas properties can be known after the experiment. Figure 9 shows the drawing and the photos of the designed venturi and U-tube manometer for gas flow rate measurement. The respective diameters are 16.5 mm and 51 mm at positions (1) and (2).

According to equations (5) and (6), the volumetric and mass flow rates of the producer gas as a function of height, *h*, are shown as equations (11) and (12). The volumetric flow rates and mass flow rates in terms of *h* are displayed in Table 1.

$$\dot{V} = 1\,728\sqrt{\mathrm{h}}\ (\mathrm{L/min}) \tag{11}$$

$$\dot{m} = 113\sqrt{\mathrm{h}}\ (\mathrm{L/min}) \tag{12}$$

5. Recorded combustion pressures and engine fan blades in terms of millisecond

After the combustion pressure acquisition system had been installed, the experimental work was conducted to test the system. The raw data are shown in Figure 10. The blue and red profiles are the combustion pressure and the detected fan blades in voltage values, respectively. However, analysts are able to understand combustion characteristics after the raw data are converted into combustion pressure in terms of the crank angle. First, we must know the cylinder pressure profile of the engine in terms of crank angle without combustion, and this baseline profile can be gained from the engine manual. After that, we identify the factor value of how to convert voltage value into the bar value of the combustion pressure. As mentioned earlier, the combustion pressure and detected fan blades were simultaneously recorded with regard to the millisecond. The rotation of one round is equal to 360º of the crank angle. Finally, we use Microsoft Excel spreadsheets to convert the fuel combustion pressure from voltage values into bar values in terms of crank angle, as shown in Figure 11. The combustion profile in Figure 11 is an example of the neat diesel mode operation at 53% engine load and 3,000 rpm engine speed.

6. Combustion characteristics

After installing the combustion pressure measurement system, the diesel engine was connected to the gasifier unit to run the engine on producer gas-diesel dual fuel mode.

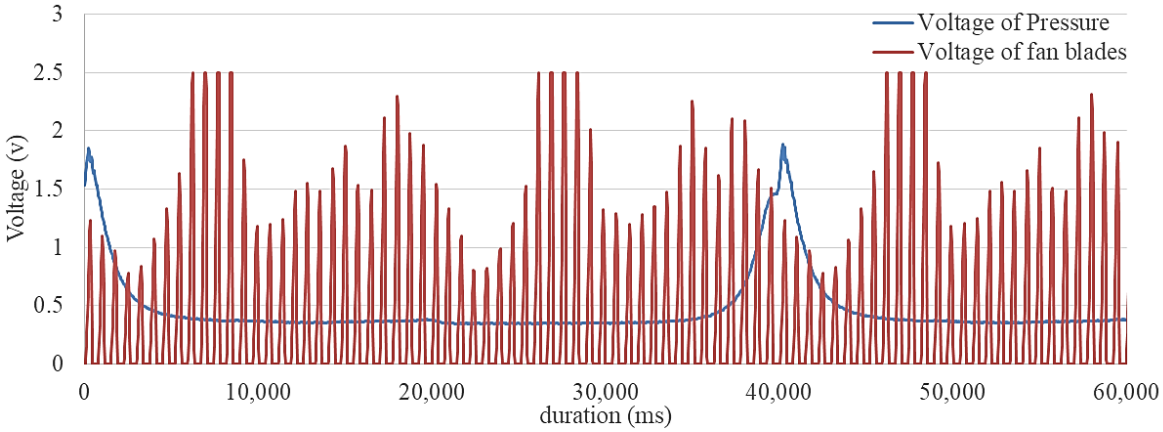

Figure 10 Raw data of combustion pressure measures and detected fan blades in voltage

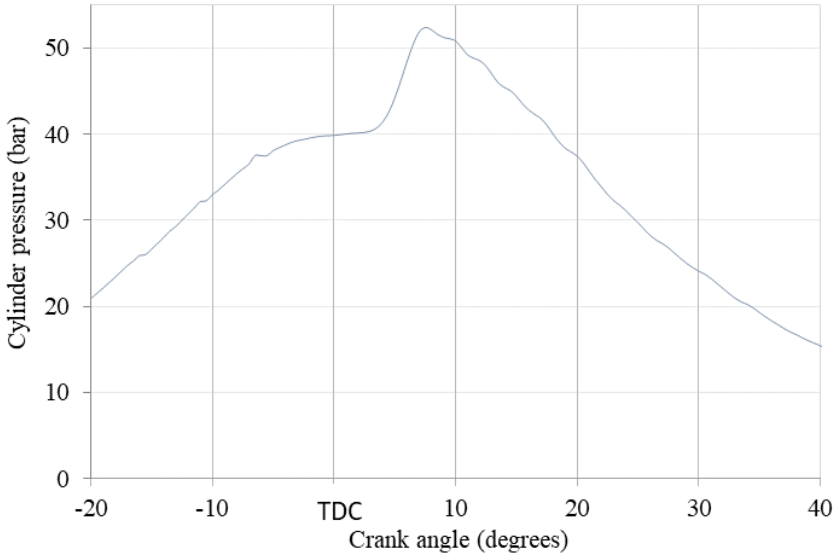

Figure 11 Fuel combustion pressure in bar value in terms of crank angle

Jatropha seed was used as the feedstock for the gasifier. The Jatropha-derived producer gas was introduced into the engine to partially replace diesel. Three different producer gas (PG) flow rates (i.e., zero gas, 10 kg/h, and 20 kg/h) and three different engine loads (i.e., 35%, 53%, and 70%) were controlled. The zero gas flow rate refers to the neat diesel operation mode. The producer gas flows through the designed venturi, and a ball valve was used to control the flow rates. A U-tube manometer was used to read gas flow rates (see Figure 9 and Table 1). The schematic diagram of the experimental setup is illustrated in Figure 12. The engine was operated at a constant engine speed of 3,000 rpm and an injection timing of 9 degrees before top dead center (BTDC).

The combustion pressure profiles are illustrated in Figure 13. The pressure profiles were the average of 20 consecutive cycles of combustion. As apparent from the figure (left side), the combustion peak occurred lower and later with an increase in gas flow rate due to an increased ignition delay during the premixed combustion phase. The same findings were reported [13, 20]. An increase in engine load improves the peak pressure as a result of an increased pilot diesel quantity that expands the ignition sources and centers (see Figure 13, right side). It was also corroborated in [13, 15].

The combustion pressure in terms of crank angle is the prerequisite used to calculate other combustion output variables, i.e., net heat release rate (NHRR) and cumulative heat release (CHR).

The NHRR is calculated using the equation below [21]:

$$\frac{dQ_n}{d\theta} = \frac{\gamma}{\gamma-1} p \frac{dV}{d\theta} + \frac{1}{\gamma-1} V \frac{dp}{d\theta} \quad (13)$$

where p is in-cylinder pressure, V is cylinder volume, $\frac{dQ_n}{d\theta}$ is NHRR (J/degree), γ is specific heat ratio $\left(\frac{C_p}{C_v}\right)$, and θ signifies crank angle (degree). The cylinder volume in terms of the crank angle is shown in Appendix 4.

Figure 14 presents the NHRR profiles. As evident from the figure (left side), the NHRR peak occurred highest and earliest for the zero producer gas flow rate. The peak occurred later with an increase in gas flow rate. The same empirical finding was also seen in [13, 15]. After the NHRR peak, the net heat release rate was observed higher with an increase in gas flow rate. This implied that the producer gas was combusted during the diffusion combustion phase due to an increased ignition delay period [1, 13, 20]. As can be seen from Figure 14 (right side), the NHRR peak was found

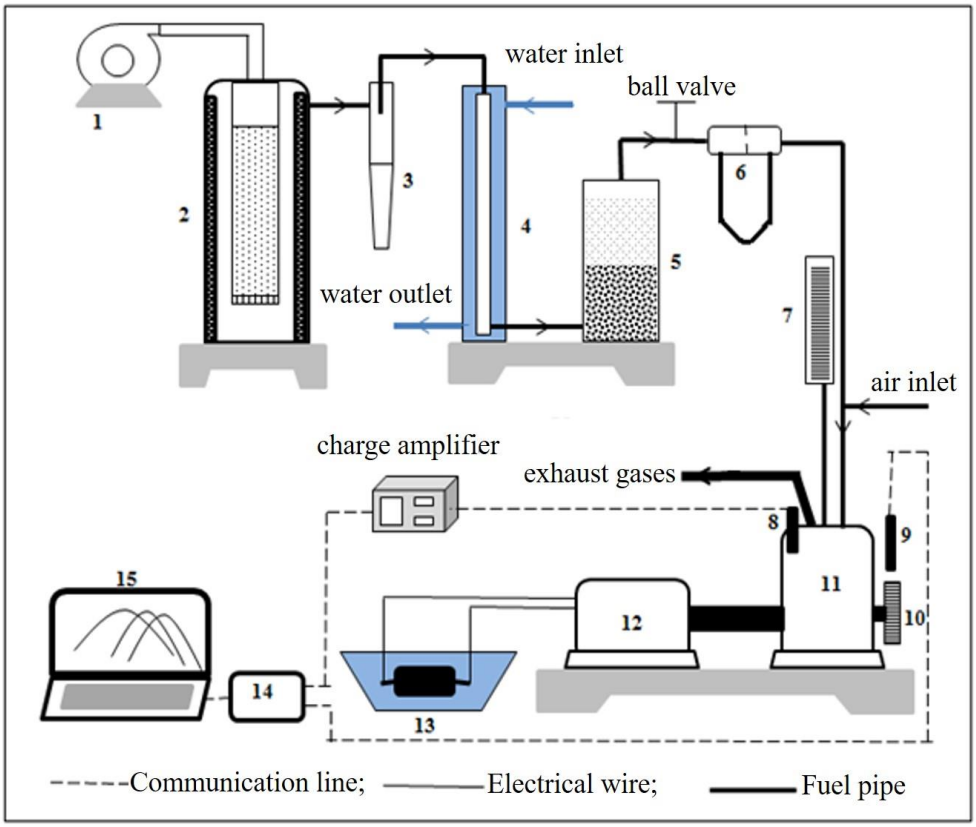

Figure 12 Schematic diagram of the gasifier-engine system: 1. Air blower, 2. Gasifier, 3. Cyclone filter, 4. Heat exchanger, 5. Dried-bed filter, 6. Venturi and U-tube manometer, 7. Diesel glass burette, 8. Pressure transducer, 9. Inductive speed sensor, 10. Engine fan blades, 11. Diesel engine, 12. Electrical alternator, 13. Water heater, 14. Data logger, 15. Laptop

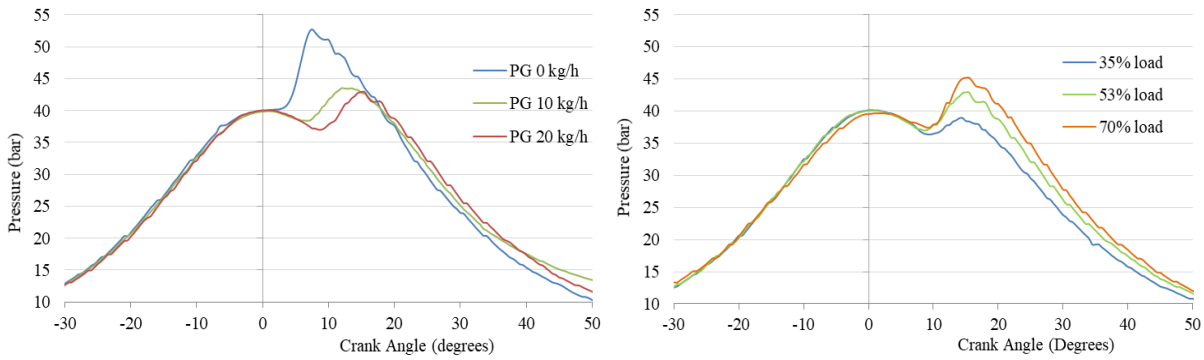

Figure 13 Combustion pressure: engine load = 70% (left) and gas flow rate = 10 kg/h (right)

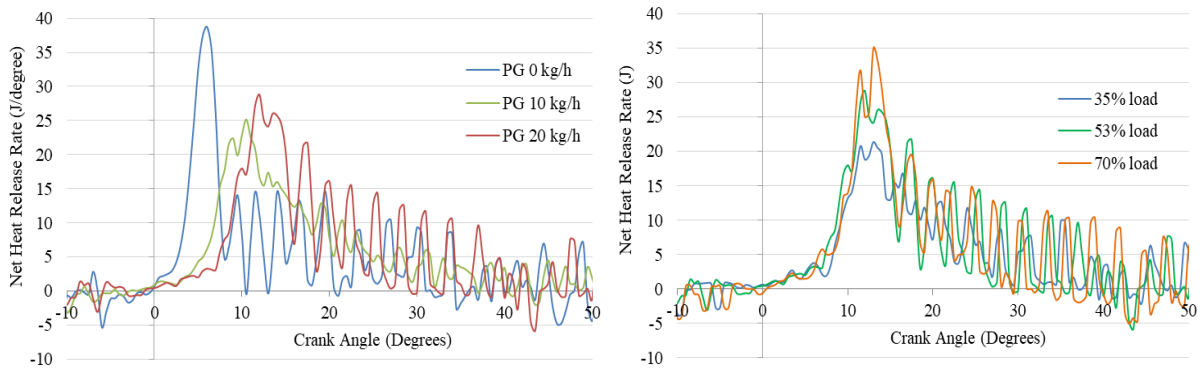

Figure 14 Net heat release rate: engine load = 70% (left) and gas flow rate = 10 kg/h (right)

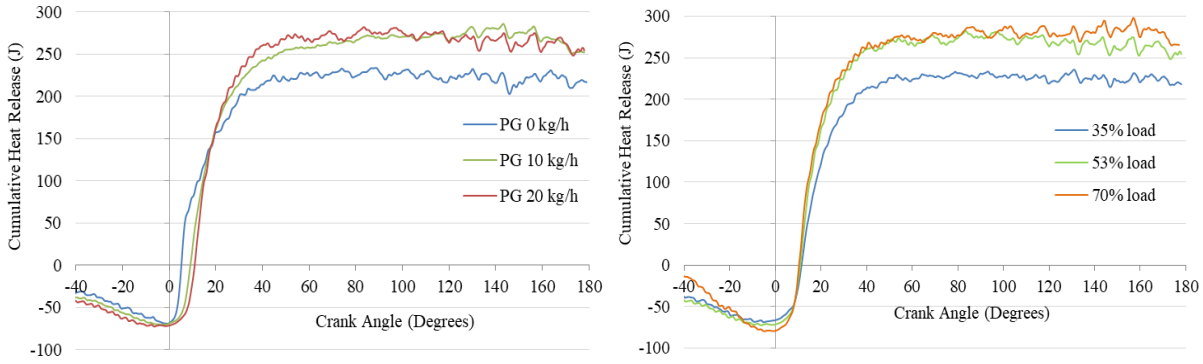

Figure 15 Cumulative heat release: engine load = 70% (left) and gas flow rate = 10 kg/h (right)

higher with an increase in engine load on account of an increased pilot diesel as the ignition source. The same finding was found in the studies of [13, 15].

Cumulative heat release (CHR) is calculated from the integration of NHHR with respect to the crank angle [6]. Figure 15 depicts the CHR in terms of the crank angle. As shown in the figure (left side), the CHR was found higher for the neat diesel mode during the premixed combustion phase due to late combustion of the dual-fuel mode. However, the CHR of the neat diesel mode was found lower during the diffusion combustion phase, as compared to the dual-fuel mode. The same finding was found in [13]. The CHR profiles of the dual-fuel modes were observed higher than that of the neat diesel mode. This indicates an excessive use and inefficiency of producer gas combustion in the dual-fuel mode. See Figure 15 (right side), the CHR of dual fuel mode was observed higher with increased engine load. The CHR profiles of 53% and 70% engine loads were very comparable. This implies that the dual-fuel engine should be operated at the maximum engine load but not at the maximum gas flow rate to minimize dual-fuel combustion inefficiency.

7. Conclusions and recommendations

This technical article provides some technical tips to design a low-cost research facility (i.e., an assembly of a combustion pressure measurement system and a gaseous fuel flow reader) for the study of combustion characteristics of producer gas on dual fuel mode. An AutoPSI pressure sensor connected with a charge amplifier and a PicoLog 1012 data logger was installed, and the total cost was 2,250 US$ only. A venturi and a U-tube manometer were designed and fabricated to read producer gas flow rates based on the Bernoulli principle. After installing the combustion pressure measurement system and the gas flow rate reader, the engine was operated at different producer gas flow rates (i.e., no gas, 10 kg/h, and 20 kg/h) and engine loads (i.e., 35%, 53%, and 70% loads) to test the installed toolkit. The results highlighted that the empirical findings of this study are very comparable with those of existing literature. The combustion pressure peak occurred lower and later with an increase in gas flow rate, but the peak was found higher when the engine load increased. The NHRR of the dual-fuel mode was found lower during the premixed combustion phase but higher during the diffusion combustion phase, compared to the neat diesel mode. The CHR was observed higher for the dual fuel mode relative to the neat diesel mode during the diffusion combustion phase, which implied less efficient combustion of the dual-fuel mode.

This technical article is informative for graduate students and academics having research budget constraints (specifically in developing countries) to study the technical feasibility of combustion characteristics of alternative fuels. Furthermore, the concept of designing the producer gas flow reader can also be generalized for other gaseous fuels such as biogas, LPG, and mixed-gases. Future research should focus on the technical feasibility of gaseous fuel converted from various biomass types through different technologies to increase the capacity of agro-waste utilization.

8. Acknowledgments

The authors are deeply grateful to two anonymous reviewers for critically reading and giving helpful comments on the manuscript's first draft. This research was funded by the Japan International Cooperation Agency (JICA) under the AUN/SEED-Net Project for a Master's Degree program at De La Salle University, the Philippines.

9. References

[1] Yilmaz H, Yilmaz I. Combustion and emission characteristics of premixed CNG/H2/CO/CO2 blending synthetic gas flames in a combustor with variable geometric swirl number. Energy, 2019;172(1):117-33.

[2] Sutheerasak E, Pirompugd W, Sanitjai S. Performance and emissions characteristics of a direct injection diesel engine from compressing producer gas in a dual fuel mode. Eng Appl Sci Res. 2018;45(1):47-55.

[3] Kalsi SS, Subramanian KA. Experimental investigations of effects of hydrogen blended CNG on performance, combustion and emissions characteristics of a biodiesel fueled reactivity controlled compression ignition engine (RCCI). Int J Hydrogen Energ. 2017;42(7):4548-60.

[4] Rith M, Biona JBM, Gitano-Briggs HW, Sok P, Gonzaga J, Arbon N, et al. Performance and emission characteristics of the genset fuelled with dual producer gas–diesel. The DLSU Research Congress; 2016 Mar 7-9; Manila City, Philippines.

[5] Kim TY, Park C, Oh S, Cho G. The effects of stratified lean combustion and exhaust gas recirculation on combustion and emission characteristics of an LPG direct injection engine. Energy. 2016;115(1):386-96.

[6] Mustafi N, Raine R, Verhelst S. Combustion and emissions characteristics of a dual fuel engine operated on alternative gaseous fuels. Fuel. 2013;109:669-78.

[7] Banapurmath NR, Tewari PG. Comparative performance studies of a 4-stroke CI engine operated on dual fuel mode with producer gas and Honge oil and

its methyl ester (HOME) with and without carburetor. Renew Energ. 2009;34:1009-15.
[8] Rith M, Arbon N, Biona JB. Optimization of diesel injection timing, producer gas flow rate, and engine load for the diesel engine operated on dual fuel mode at a high engine speed. Eng Appl Sci Res. 2019;46(3):192-9.
[9] Gao J, Tian G, Sorniotti A. On the emission reduction through the application of an electrically heated catalyst to a diesel vehicle. Energy Sci Eng. 2019;7(6):2383-97.
[10] Gao J, Tian G, Sorniotti A, Karci AE, Palo RD. Review of thermal management of catalytic converters to decrease engine emissions during cold start and warm up. Appl Therm Eng. 2019;147:177-87.
[11] Rith M, Gitano-Briggs HW, Arbon NA, Gonzaga JA, Biona JBM. The effect of Jatropha seed cake producer gas flow rates on a diesel engine operated on dual fuel mode at high engine speed. Eng Appl Sci Res. 2019;46(4):303-11.
[12] Rith M, Biona JBM, Maglaya AB, Fernando A, Gonzaga JA, Gitano-Briggs HW. Fumigation of producer gas in a diesel genset: Performance and emission characteristics. 10th International Conference on Humanoid, Nanotechnology, Information Technology, Communication and Control, Environment and Management (HNICEM); 2018 Nov 29 – Dec 2; Baguio City, Philippines. USA: IEEE; 2019. p. 1-4.
[13] Rith M, Buenconsejo B, Gonzaga JA, Gitano-Briggs HW, Lopez NS, Biona JBM. The combustion and emission characteristics of the diesel engine operated on a dual producer gas-diesel fuel mode. Eng Appl Sci Res. 2019;46(4):360-70.
[14] Rith M, Gitano-Briggs HW, Gonzaga JA, Biona JBM. Optimization of control factors for a diesel engine fueled with jatropha seed producer gas on dual fuel mode. Int Energ J. 2019;19(3):149-58.
[15] Sombatwong, P, Thaiyasuit P, Pianthong K. Effect of pilot fuel quantity on the performance and emission of a dual producer gas-diesel engine. Energy Procedia. 2013;34(2013):218-27.
[16] Raheman H, Padhee D. Combustion characteristics of diesel engine using producer gas and blends of Jatropha methyl ester with diesel in mixed fuel. Int J Renew Energ Dev. 2014;3(3):228-35.
[17] Banapurmath NR, Tewari PG, Hosmath RS. Experimental investigations of a four-stroke single cylinder direct injection diesel engine operated on dual fuel mode with producer gas as inducted fuel and Honge oil and its methyl ester (HOME) as injected fuels. Renew Energ. 2008;33(2008):2007-18.
[18] Optrand Incorporated. Optrand introduces a combustion analyzer for its cylinder pressure sensors [Internet]. 2018 [cited 2020 May 5]. Available from: http://www.optrand.com/.
[19] Rith M, Buenconsejo B, Biona JBM. Design and fabrication of a downdraft gasifier coupled with a small-scale diesel engine. Eng Appl Sci Res. 2020;47(1):117-28.
[20] Kreith F, Manglik RM, Bohn MS. Principles of heat transfer. 6th ed. USA: Global Engineering; 2011.
[21] Heywood J. Internal combustion engine fundamentals. New York: McGraw-Hill; 1988.
[22] Pico Technology. PicoLog 1000 Manuals [Intermet]. 2019 [cited 2020 May 5]. Available from: https://www.picotech.com/data-logger/picolog-1000-series/picolog-1000-manuals.

Appendix 1 Specifications of the AutoPSI Pressure Sensor [17]

Item	Description
Over pressure	2 X Pressure Range (typical)
Non-linearity and hysteresis	$\pm$ 0.5% FS under non-combustion condition, under constant temperature $\pm$ 1% FS under combustion conditions, i.e., varying temperature within one combustion cycle
Diaphragm resonant frequency	120 kHz min
Frequency range	1.0 Hz to 25 kHz
Sensor housing temperature range	$-40℃$ to $380℃$
Cable operating temperature	$-40℃$ to $200℃$
Fiber optic cable length	1.5m (5′)
Fiber optic cable min Bending radius	5mm (3/16″)
Sensor type	Sealed gauge
Interface unit	Integrated with sensor
Pressure output signal (Analog)	$9-18$V DC input: $0.5-4.5$ V 5V DC input: $0.5-4.5$V
Diagnostic output signal (Analog)	$9-18$V DC input: $0.5-2.5$ V 5V DC input: $0.5-4.5$V
Power supply voltage	$9-18$V DC or 5V DC
Current draw	85 mA Max, 50 mA Typical
Interface temperature range	AutoPSI-S, A, TC: $-20℃$ to $60℃$ AutoPSI-S, A, TC: $-20℃$ to $125℃$
Pressure media	Gaseous or Liquid
Vibration	100G
Guaranteed lifetime	1, 2, or 3 years

Appendix 2 Main specifications of the engine

Item	Description
Model	KM 186F
Engine type	Single cylinder, 4-stroke, air-cooled, direct injection, naturally aspirated, diesel engine
Bore×stroke	86×70 (mm)
Connecting rod length	117.5 (mm)
Displacement	406 (cm^3)
Compression ratio	19:1
Diesel injection timing	BTDC 9° of crake angel
Rated output power	5.7 (kW)
Engine speed	3,000 (rpm)

Appendix 3 Specifications of a PicoLog 1000 Series, 1012 Modal, Data Logger [22]

Item	Description
Maximum Sampling Rate	
Continuous streaming	100 kS/s single-channel
Block mode	1MS/s single-channle
Buffer Size	8k samples, shared by all channels
Analog Inputs	12
Analog Bandwidth (−3dB)	DC to 70 kHz
Input Type	Single-ended, unipolar
Input Voltage Range	0to +2.5V
Linearity (at 25℃)	1LSB
Resolution	10 bits
Accuracy	1%
Overload Protection	± 30 V to ground
Input Coupling	DC
Input Impedance	1 MΩ
Digital Outputs (D0 ... D3)	2
Digital Outputs (PWM)	None
Period	100µs to 1 800µs
Duty Cycle	Adjustable from 0% to 100% in 1% steps
Digital Output (all)	
Logic Low Voltage	100 mV (typical)
Logic High Voltage	3.3 V
Current Limiting	1 kΩ resistors in series with outputs
Power Output for Sensors	2.5 V @ 10 mA, current-limited
Ground Fault Current Protection	0.9 A thermal self-resetting fuse
I/O Connector	25-way D female
Environmental Operating Condition	
For Quoted Accuracy	20℃ to 50℃ for quoted accuracy
General Operation	0℃ to 70℃ overall
Relative Humidity	50℃ to 80℃ RH
Compliance	CE (EMC) class A emissions & immunity FCC emissions
PC Connection	USB 2.0
Dimensions	45 mm × 1000mm × 140 mm (1.77" × 3.94" × 5.51")
Weight	< 200 g (7.05 oz)

Appendix 4 Volume of engine cylinder in terms of crank angle

$$V(\theta) = V_C + V_D = V_c + \pi\frac{D^2}{4}X(\theta)$$

$$X(\theta) = (L - L') + (r - r')$$

$$\text{But } r' = r\cos\theta \qquad r'' = r\sin\theta \qquad L' = \sqrt{L^2 - (r\sin\theta)^2}$$

$$X(\theta) = L\left(1 - \sqrt{1 - \left(\frac{r}{L}\sin\theta\right)^2}\right) + r(1 - \cos\theta)$$

$$\Rightarrow V(\theta) = V_c + \pi\frac{D^2}{4}\left[L\left(1 - \sqrt{1 - \left(\frac{r}{L}\sin\theta\right)^2}\right) + r(1 - \cos\theta)\right]$$